

REPORT DOCUMENTATION PAGE			<i>Form Approved</i> <i>OMB No. 074-0188</i>	
Public reporting burden for this collection of information is estimated to average 1 hour per response, including the time for reviewing instructions, searching existing data sources, gathering and maintaining the data needed, and completing and reviewing this collection of information. Send comments regarding this burden estimate or any other aspect of this collection of information, including suggestions for reducing this burden to Washington Headquarters Services, Directorate for Information Operations and Reports, 1215 Jefferson Davis Highway, Suite 1204, Arlington, VA 22202-4302, and to the Office of Management and Budget, Paperwork Reduction Project (0704-0188), Washington, DC 20503				
1. AGENCY USE ONLY (Leave blank)	2. REPORT DATE 7/30/2010 (FINAL)	3. REPORT TYPE AND DATES COVERED Performance 11/1/2006 - 4/30/2010		
4. TITLE AND SUBTITLE Ultrashort Intense Pulse Propagator Applications: Light Strings, Higher Harmonic Generation and Extreme NLO			5. FUNDING NUMBERS FA9550-07-1-0010	
6. AUTHOR(S) PI: Jerome V Moloney Co_PI: Miroslav Kolesik				
7. PERFORMING ORGANIZATION NAME(S) AND ADDRESS(ES) Arizona Board of Regents University of Arizona 888 N. Euclid Avenue, Room 510 Tucson, Arizona 85722-3308			8. PERFORMING ORGANIZATION REPORT NUMBER FA9550-07-1-0010	
9. SPONSORING / MONITORING AGENCY NAME(S) AND ADDRESS(ES) USAF AF Office of Scientific Research 875 North Randolph Road, Suite 325 Arlington, VA 22203			10. SPONSORING / MONITORING AGENCY REPORT NUMBER N/A AFRL-OSR-VA-TR-2012-0609	
11. SUPPLEMENTARY NOTES N/A				
12a. DISTRIBUTION / AVAILABILITY STATEMENT Unclassified and Unlimited-A			12b. DISTRIBUTION CODE	
13. ABSTRACT (Maximum 200 Words) Our optical carrier-resolved unidirectional Maxwell solver for propagating ultrashort pulses in air and condensed media continues to be employed to study extreme nonlinear optical effects in such media. Specific highlights include modification and extension of plasma channels in air using ultra-intense pulses with transverse Bessel and Airy beam profiles. A joint theory and experimental study using Bessel beams to extend and Airy beams to extend and bend plasma channels in air has led to wide exposure in both the scientific literature and in the news media. We are currently theoretically investigating generation of generalized conical beam pulses which allow for independent control of on-axis intensity and phase evolution. As an example of such control, we have studied usage of "polarization gating," utilizing a highly birefringent hollow-core fiber model, to achieve highly efficient quasi-phase matching for third harmonic generation. We continue to develop FDTD vector Maxwell solvers based on an adaptive space-time meshing algorithm and are incorporating non-orthogonal meshes to remove staircase effects on near-fields computed on abrupt material interfaces of arbitrary shape. individual nanoparticles, quantum dots etc.				
14. SUBJECT TERMS			15. NUMBER OF PAGES 24	
			16. PRICE CODE	
17. SECURITY CLASSIFICATION OF REPORT	18. SECURITY CLASSIFICATION OF THIS PAGE	19. SECURITY CLASSIFICATION OF ABSTRACT	20. LIMITATION OF ABSTRACT	
	U	U	n/a	

Ultrashort Intense Pulse Propagator Applications: Light Strings, Higher Harmonic Generation and Extreme NLO

Final Technical Report

Executive summary

Our optical carrier-resolved unidirectional Maxwell solver for propagating ultra-short pulses in air and condensed media continues to be employed to study extreme nonlinear optical effects in such media. Specific highlights include modification and extension of plasma channels in air using ultra-intense pulses with transverse Bessel and Airy beam profiles. A joint theory and experimental study using Bessel beams to extend and Airy beams to extend and bend plasma channels in air has led to wide exposure in both the scientific literature and in the news media. We are currently theoretically investigating generation of generalized conical beam pulses which allow for independent control of on-axis intensity and phase evolution. As an example of such control, we have studied usage of “polarization gating,” utilizing a highly birefringent hollow-core fiber model, to achieve highly efficient quasi-phase matching for third harmonic generation.

We continue to develop FDTD vector Maxwell solvers based on an adaptive space-time meshing algorithm and are incorporating non-orthogonal meshes to remove staircase effects on near-fields computed on abrupt material interfaces of arbitrary shape. Novel approaches have been developed to accurately compute the far-field distribution from numerical near-fields and to accurately compute tiny forces (nano-Newtons) on individual nanoparticles, quantum dots etc.

Personnel Supported:

PI: J. V Moloney

Co-PI: M. Kolesik

Faculty:

M. Brio

C. Dineen

J. Hader

S.W. Koch

P. Polynkin

P. Jakobsen

S.W. Koch

E.M Wright

Postdoctoral Fellows:

Y. Zeng

J. Liu

M. Yarborough

Y. Bae

A.S Bhullar

E. Kashdan

Graduate Students:

G. Hardesty
 Y. Lai
 D. Roskey
 T.S. Wang
 J. Gilbert
 G. Hardesty
 H.B Li
 D. Love
 J. Pate

Nonlinear Optics with Shaped Beams

Pulsed Airy beams and curved plasma channels.

There has been a lot of work done in the general area of Airy beams concentrated on their exotic linear propagation properties. We were the first group to extend these studies into the nonlinear regime. In our work published recently in Science, we have studied filaments created in high-power, pulsed Airy beams. We have shown, in experiment and through a large-scale numerical simulations, that the bending properties of linear Airy beams do indeed translate into bent filaments and plasma channels. The experimental set-up is depicted in the

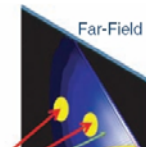


Fig. 1. Experimental setup. The continuous wave visible laser beam that we used as a spatial reference has a much smaller size than that of the phase mask. The reference beam experiences

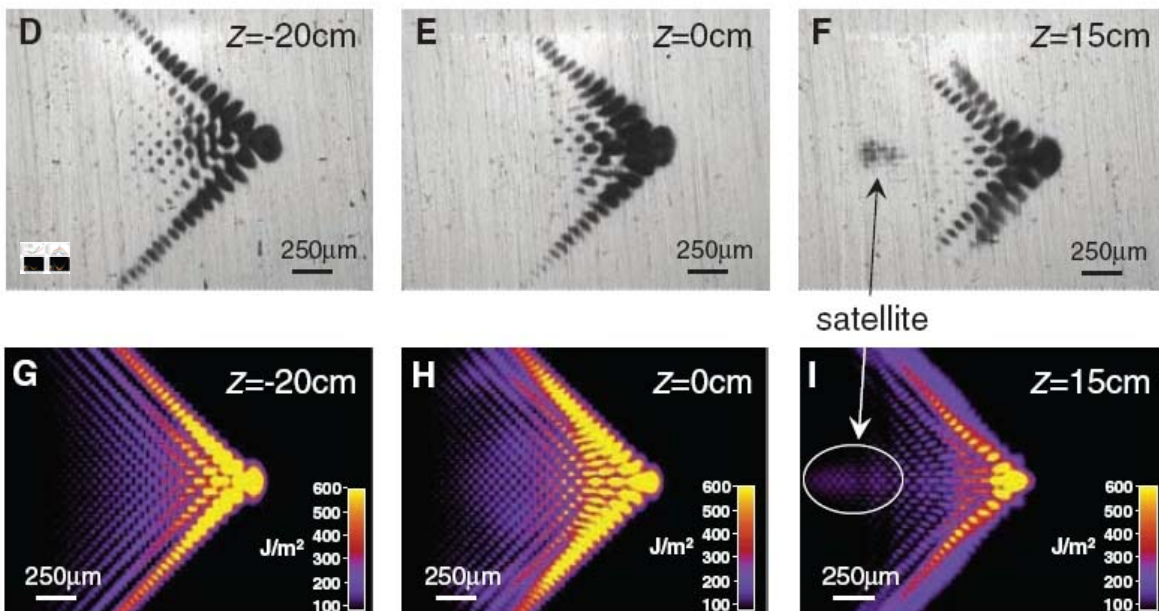
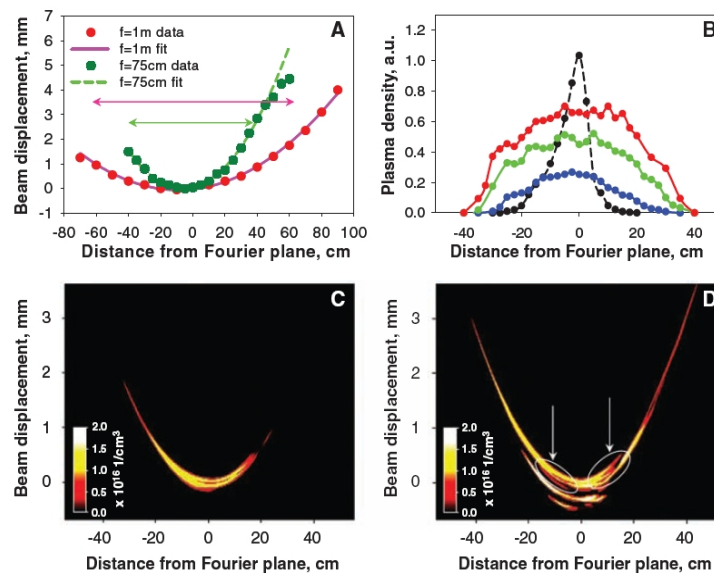


Fig. 4. Near-field beam patterns at different locations along the propagation direction. (A to C) Burn patterns on an aluminum foil for 5-mJ pulses. No apparent satellite is formed in the transverse plane during propagation. (D to F) Same as in (A) to (C) but for 10-mJ pulses. The beam undergoes a nonlinear reshaping, and a satellite spot appears that is indicated by the arrow in image F. (G to I) Numerically simulated near-field intensity profiles for 10-mJ pulses. Both the whisker-shaped ghost beam and the faint satellite are visible in (I).

figure on the right: A phase mask imposes a cubic phase profile on a Gaussian beam, which then passes through a lens and subsequently forms an Airy beam profile around the focal spot of the lens. The Airy profile is a two-dimensional direct product of Airy functions, each for one transverse dimension. This is illustrated in the Figure at the bottom of this page. The upper rows shows experimental “burn patters” left by the beam in an aluminum foil. In the Panel F it can be seen that the nonlinear propagation resulted in reshaping of the energy fluence profile, while the characteristic 2D Airy pattern remained preserved. A very similar behavior has been observed in our numerical simulations depicted in the lower row. This tells us that the model can be trusted to investigate also those properties which are not directly observable in the experiment. In particular we were interested in the shape of the plasma channels generated in the filament. So far all plasma channels observed in femto-second filamentation were straight, although in principle a plasma channel “fusion” should be possible in situation with multiple filaments and when two or more filaments join into one along their propagation. Here we have the possibility that a nontrivial plasma distribution is created in a single filament, provided that at least some remnants of linear propagation properties of the Airy beam can survive the influence of nonlinear interactions. And this is indeed what we have found. Some of our experimental and simulation results are illustrated in the following Figure.



Panel A depicts the measured geometry of the curved path of the Airy beam intensity maximum, while Panel B shows the measured plasma density along this “trajectory.” The bottom Panels are simulation results for the plasma (electron) number density, demonstrating the bent character of the Airy beam plasma channel. At lower pulse energies, the plasma channel essentially follows the parabolic trajectory of the airy beam maximum. The non-linear propagation results only in a slight renormalization or straightening of the parabola (indiscernible on this scale). At a higher power, plasma channels still bend, but can bifurcate at places where the central lobe of the beam suffers from a local self-focusing collapse. These are locations akin to repeated self-focusing collapses and subsequent beam revivals in “standard” femtosecond filaments. We have thus demonstrated, for the first time, that there is a potentially very useful interplay between the linear and nonlinear properties of pulsed Airy beams.

Airy beam filamentation in water

Our previous studies of femtosecond filamentation dynamics in dispersive media, including water, have shown that angularly resolved spectra, or far field spectra, present a very useful tool to uncover the dynamics in the core of the filament. Specifically, it is possible to judge, based on the “topology” or two-dimensional shape of the far-field spectrum if a pulse splitting occurred. It is also possible to extract the daughter peak velocities, or rate

at which the splitting happened. Often it is also possible to infer the asymmetry of the splitting event, and namely to say which of the daughter pulses dominated. It was also shown that each of the self-focusing and replenishment cycles gives rise to a contribution in the far field. As a result, for a straight filament, characteristic X-shaped features of the far-field spectra tend to overlap and produce interference patterns which in turn severely impair the possibility to extract any quantitative information from the angular spectrum. This is where Airy pulsed beams become interesting: As discussed above, the trajectory along which the main intense lobe of the pulse propagates, even in the presence of non-linearity, is a parabola. Thus if two self-focusing collapses occur at distinct loci along this path, one can ask if it is possible that the conical emission and supercontinuum in general will follow the tangent direction, and thus will separate in the far field. If this was the case, far-field snapshots corresponding to different points along the propagation distance could be distinguished. Then, the far-field spectra could give us a tool to probe if the subsequent collapses followed the same scenario, or if the propagation distance matters. Such was the motivation of our work published recently in Physical Review Letters, which is briefly reviewed in what follows. The scheme of the experiment is shown in the Figure:

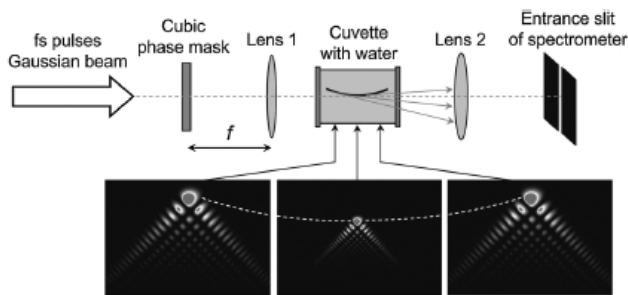


FIG. 1. Schematic of the experiment. The dominant lobe of the Airy beam pattern travels along a parabolic trajectory, as illustrated by the series of three intensity patterns in the bottom part of the figure.

A pulsed Airy beam is formed within a water cell in which edges can be accurately placed to form obstacles for light propagation, and thus select portions of the radiative patterns to be analyzed downstream on the exit from the cell. There, the far field spectrum is measured by an imaging spectrometer and recorded by a digital camera. If an aperture is inserted in such a way that only the center of the filament passes through, the subsequent filamentation is canceled due to the absence of the low-

intensity background which, as we have shown some years ago, feeds the filament core formation. Then, in the radiation collected in the far field will reflect the self-focusing collapse in the close vicinity of the screen. If on the other hand, and edge is inserted such that the very central lobe of the beam is “killed”, we have a situation when the subsequent filamentation is largely undisturbed because it forms of the low intensity background left intact by the screen edge. This is depicted in the following Figure, which also shows digital camera pictures of the far field.

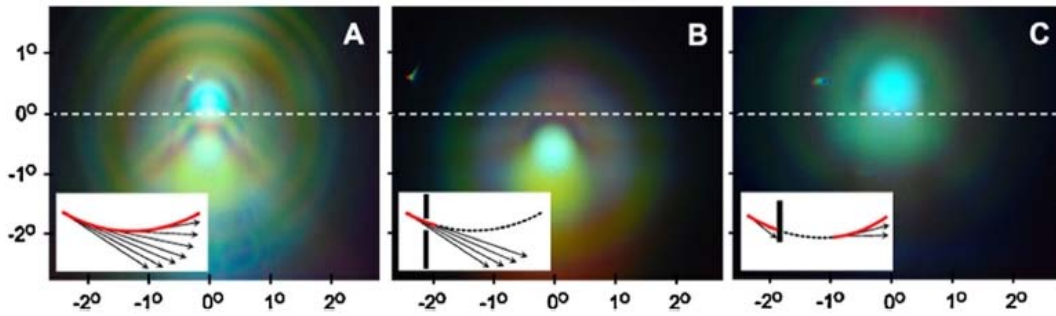


FIG. 2 (color online). Photographs of the forward emission patterns by bent filament. The insets illustrate how the emission originating from different sections of the filament is isolated from the rest of the emission. (a) Complete emission pattern. (b) Emission pattern from the beginning section of the filament. (c) Emission pattern from the end section of the filament.

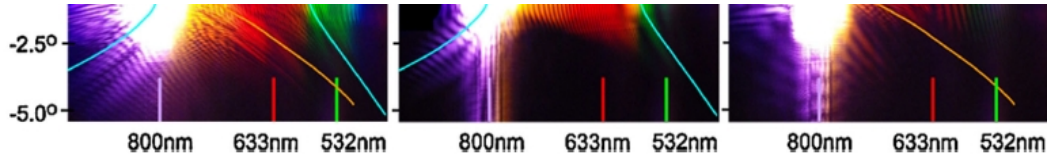


FIG. 3 (color online). θ - λ spectral maps of the forward supercontinuum emission. (a) Complete emission pattern. (b) Emission from the beginning section of the filament. (c) Emission from the end section of the filament. In figures (b) and (c), the best-fit curves based on the effective three-wave mixing approach are shown with light blue and orange solid lines. Same best-fit curves are also shown in the complete pattern (a).

It can be clearly seen that the conical emission produced at different locations along the parabolic beam trajectory is directed along the tangent to this parabola. Thus, as indicated above, it is indeed possible to separate, at least partially, the white-light generation signatures originating in distinct spots. Now we can turn to the question if one can utilize the far field spectra of the radiation shown above to say anything about the dynamics of the Airy filament. The next Figure shows three different far field spectra:

The first panel is a total spectrum, and it clearly reveals a “superposition” of two patterns. These are then separated, in the way described above, and recorded in isolation. Indeed, the second and third panel do indicate that there is a difference in how the subsequent collapse events occur. Based on our previous results concerning the filamentation dynamics, and interpretation of far field spectral patterns we can say that the first picture corresponds to a pulse splitting event in which the trailing daughter pulse dominates strongly. The distance between the fundamental and high-frequency X-feature of the spectrum then tells about the group velocity of the post-collapse light pulse. The third panel, on the other hand, must be due to a pulse splitting event in which the leading pulse dominates. We can thus come to an experimental conclusion that the subsequent collapse events may be qualitatively different. This further refines the spatial replenishment scenario put forward by the Tucson group years ago. However, these observations also pose questions for which we do not have satisfactory answers at this point. We have shown in multiple cases, that in straight-path filaments it is possible to use the so-called Effective Three-Wave Mixing picture to characterize very accurately the loci in the spectra along which the energy of newly formed radiation accumulates. These are usually termed X-features because they are intimately connected with the conical nature of the white-light radiation. In the above picture, the long X-feature arms are clearly visible and sharply formed. However, our ETW analysis, illustrated by the fitting curves shown in the figure is far from satisfactory. This indicates to us that while the overall filamentation picture in the Airy beam follows the established scenario, the exotic nature of this waveform has consequences that will require further detailed study and careful mathematical analysis.

Nonlinear Optics With Bessel Beams.

The following sections highlight our results in the field of filamentation and high-harmonic generation control using femtosecond pulses with carefully shaped beam profiles.

Generation of extended plasma channels in air using femtosecond Bessel beams

Extending the longitudinal range of plasma channels created by ultrashort laser pulses in atmosphere is important in practical applications of laser-induced plasma such as remote spectroscopy and lightning control. Weakly focused femtosecond Gaussian beams that are commonly used for generating plasma channels offer only a limited control. Increasing the pulse energy in this case typically results in creation of multiple filaments and does not appreciably extend the longitudinal range of filamentation. Bessel beams with their extended linear foci intuitively appear to be better suited for generation of long plasma channels. Building on this idea, we reported results on creating extended filaments in air

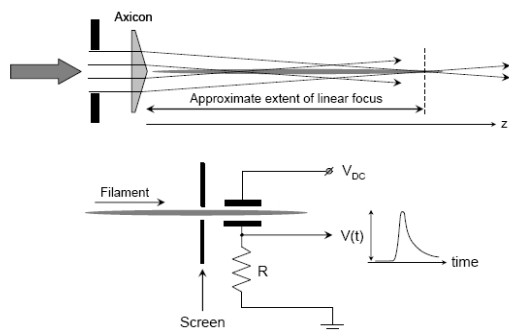


Fig. 1. Schematic of the experiment. Top: Filamentation with apertured femtosecond Bessel beam. Bottom: Setup for probing local charge density in the plasma channel.

channel can be longitudinally shifted beyond the linear-focus zone, an important effect that may potentially offer additional means of controlling filament formation. The following

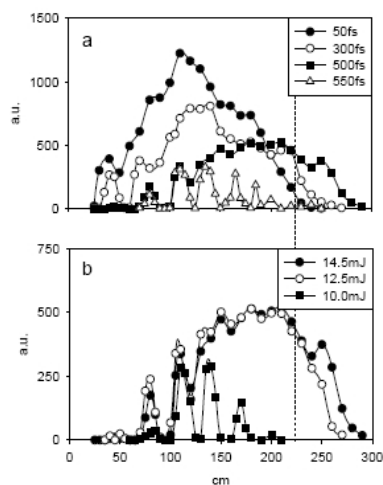


Fig. 4. a: Linear plasma density for temporally chirped femtosecond Bessel beams. Pulse energy is 14.5 mJ in all cases. Different curves correspond to different pulse widths as specified in the inset. b: Same for 500 fs-long pulse. Different curves correspond to three different values of the pulse energy as specified in the inset. Units on the vertical axes of both graphs are same as in Figs. 2(b) and 3(b).

using femtosecond Bessel beams. By probing the linear plasma density along the filament (see the figure for the schemes of Bessel beam generation and a plasma sensing probe), we show that apertured Bessel beams produce stable single plasma channels that span the entire extent of the linear focus of the beam. We further show that by temporally chirping the pulse, the plasma

channel can be longitudinally shifted beyond the linear-focus zone, an important effect that may potentially offer additional means of controlling filament formation. The following Figure shows select experimental results to illustrate this conclusion. The top panel indicates that there exists an optimal value of chirp, for which the resulting plasma channel reaches the furthest distance from the laser. The lower panel illustrates the role of the pulse energy. In particular, here we demonstrate that unlike in Gaussian beams, increasing the Bessel beam energy does not lead to multiple filaments, and the energy increase translates into a longer plasma channel.

Extended filamentation with temporally chirped femtosecond Bessel-Gauss beams in air

We experimentally studied extended filamentation with temporally chirped femtosecond Bessel-Gauss beams in air in the following setup:

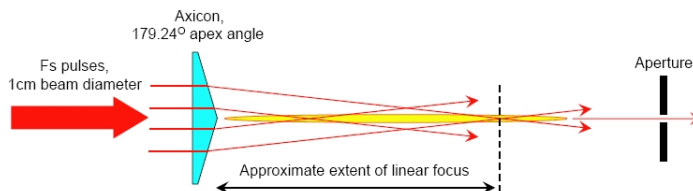


Fig. 1. Experimental setup. The aperture placed 4 m away from the axicon is used to isolate light propagating along the beam axis in the far-field.

We found that the longitudinal extent of the plasma channels is maximized for a particular duration of the chirped pulses as shown in the picture below. The next Figure shows that

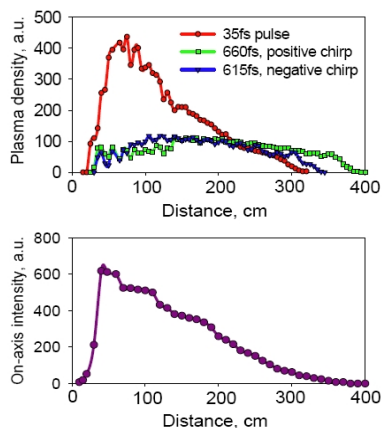


Fig. 3. Top: Linear plasma density along the filament for the fully compressed pulse and for positively and negatively chirped pulses that maximize the longitudinal extent of the plasma channel. Pulse energy is 14 mJ in all cases. Bottom: On-axis intensity of the Bessel-Gauss beam in the linear propagation regime.

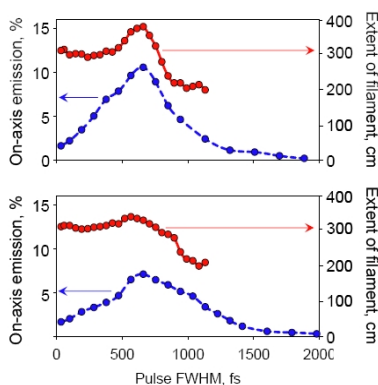


Fig. 4. Longitudinal range of the plasma channel and the fraction of the input pulse energy re-emitted by the beam along the beam axis, as functions of the FWHM pulselength. Top figure: Positively chirped pulses. Bottom figure: Negatively chirped pulses. The maximum fraction of the on-axis energy is over 10% and 7% for positively and negatively chirped pulses, respectively.

the effect was found to be related to the emission of a strong on-axis component along the beam axis that, under certain conditions, attains sufficient energy to initiate filamentation on its own. We attributed the on-axis emission by the femtosecond Bessel-Gauss beam to the nonlinear four-wave mixing process in which both signal and idler waves are emitted along the beam axis. Using plasma-assisted phase-matching considerations, we derived a simple formula that relates the pulse-length of the chirped pulse that results in longest filament, to the relevant experimental parameters. Estimates based on this formula are found to be in good agreement with the experiments, and we find a clear correlation between the extent of filamentation and the intensity of the on-axis emission by the femtosecond Bessel-Gauss beam. The on-axis emission is negligible for fully compressed pulses, but it can become quite substantial (up to 10% of the input pulse energy) when chirped pulses are used. Under certain conditions, the on-axis emission becomes sufficient for generating its own plasma channel thus resulting in extended filamentation. This effect may offer means of remote control over filament formation.

Phase matching with pulsed Bessel beams for high-order harmonic generation

We proposed a novel approach to obtain phase-matched generation of high-order harmonics based on the use of pulsed Bessel beams as pump pulses:

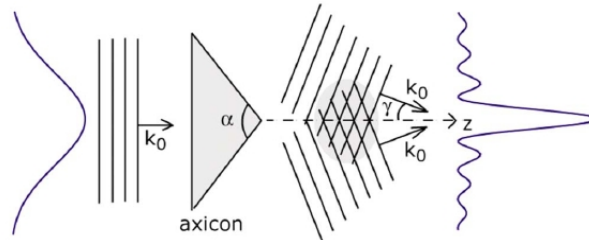


FIG. 1. (Color online) Bidimensional sketch of the generation of a PBB by sending a Gaussian pulse into an axicon. The phase fronts acquire a tilt γ . The interference between the off-axis propagating fronts creates the peculiar radial intensity distribution.

By means of the “coherence map” technique, we showed that it is possible to maximize the generation of a chosen harmonic of interest by properly adjusting the phase front tilt of the pulsed Bessel beam to compensate the mismatch arising from material and plasma dispersion and atomic phase. We demonstrated that by appropriate choice of the Pulsed Bessel Beam (PBB) parameters it is possible to effectively phase match the HHG and reach the absorption limit for any harmonic of interest as long as the pump pulse remains below the critical ionization threshold, a result that can be reached only in very specific operating conditions using Gaussian pulses, and without the limitations of a hollow waveguide.

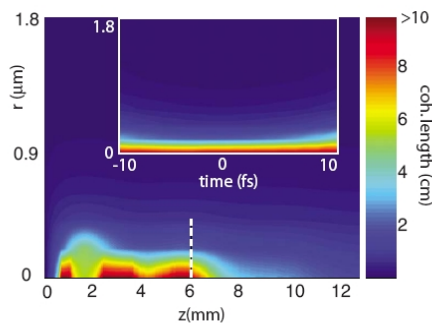


FIG. 2. (Color online) Coherence length (in cm) for a Bessel pump beam in helium phase matched with the 61st harmonic over 1 cm of propagation from the beginning of the gas cell. The inset shows the radial vs local time coherence map along the PBB profile at $z=6$ mm (dashed line).

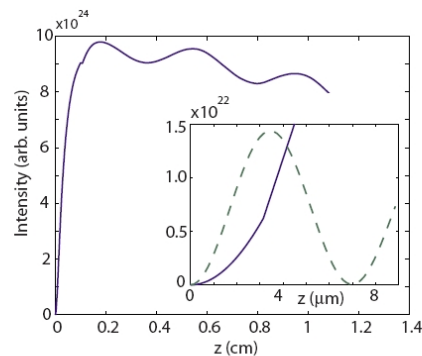
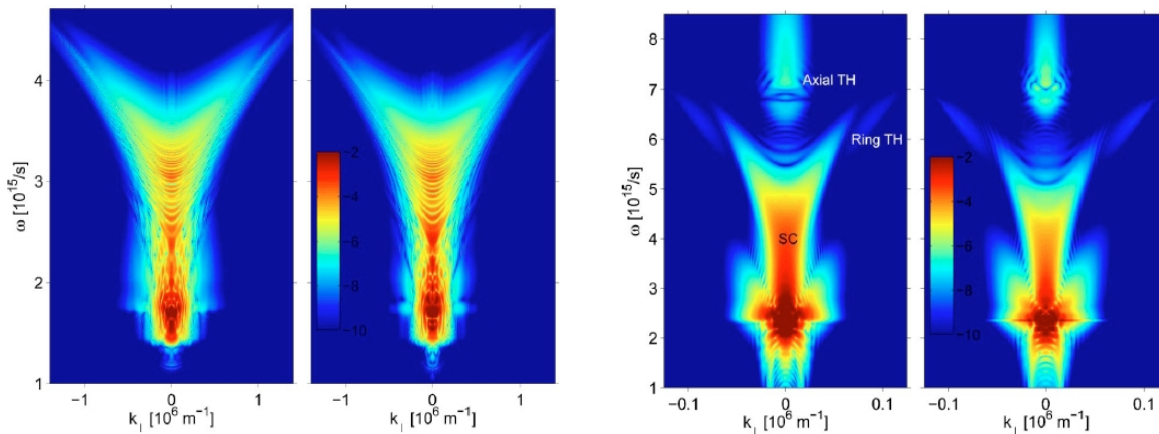


FIG. 3. (Color online) Calculated power in the 61st harmonic generated in helium using a phase matched PBB pump. The inset shows in detail the power growth in the first few microns compared to that obtained with the Gaussian pump pulse with the same input energy and peak intensity.

Moreover, since the harmonic signal remains high over a reasonable distance of several millimeters once it reaches the absorption limit, the experimental realization with a gas cell should easily be feasible. This technique was studied in specific cases in He and Ar gases but may be readily applied in other operating conditions, in particular to higher pump intensities while remaining below the critical ionization limit. Our results within the approximation of the coherence map technique give a strong indication of a new possible approach for phase matching that deserves further attention.

Supercontinuum and third-harmonic generation accompanying optical filamentation as first-order scattering processes

Through a comparative theoretic and simulation study, we demonstrated that the supercontinuum generation and third-harmonic generation that accompany optical filamentation in nonlinear dispersive bulk media can be described as first-order scattering processes akin to the first Born approximation. In particular, for an incident ultrashort pulse the angularly resolved spectrum of the transmitted pulse is shown to be accurately determined using first-order scattering of the incident field from the nonlinearly modified refractive index due to the optical filament. Thus, although an optical filament is a highly nonlinear object, the accompanying supercontinuum generation and third-harmonic generation are driven parametrically by the filament and have negligible back action upon it. The following picture illustrates this result:



The left hand side panel compares the spectrum as generated in water (anomalous GVD regime) and simulated with the full model using the UPPE solver, with the First-Born approximation. In the right-hand-side panel, a similar comparison is made for air, i.e. in the normal GVD regime. As we can see, the First-Born theory gives an extremely accurate picture of the angularly resolved white-light spectrum. We have thus shown that the first Born approximation is accurate in both normal and anomalous GVD regimes, in a condensed medium, and in air. It explains the spectral and angular distribution of both the SC and the TH radiation. This is expected to hold in general for nonlinear dispersive bulk media and in absence of resonance interactions.

Perturbative and non-perturbative aspects of optical filamentation in bulk dielectric media

The field of optical filament formation from initial ultrashort laser pulses in bulk dielectric media has now reached a high state of maturity, and has been studied in all three phases of matter, including long distance propagation in air, also termed light string propagation, water, and glass. From the earliest studies of light string propagation in air it was observed that conical emission, namely colored light emission off-axis from the filament, was a byproduct that accompanied the filamentation process. Since then several other byproducts accompanying optical filamentation have been studied, namely, white light or

supercontinuum (SC) generation, third-harmonic (TH) generation, and X- and O-waves (see illustration).

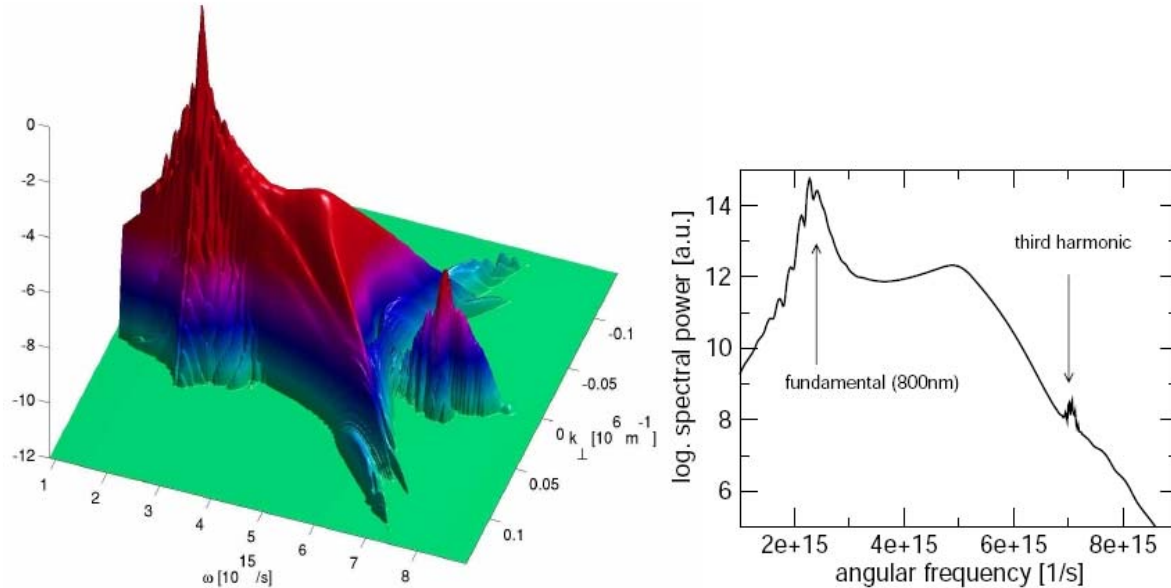


Fig. 2. Supercontinuum and third-harmonic generation in air. The right panel shows angle-integrated spectrum. The weak feature above the high-frequency background is due to third harmonic generation. The angularly resolved spectrum on the left reveals angular separation between the supercontinuum and third harmonic radiation parts of the spectrum.

In our work published in a focus issue of Optics Express, we have brought these manifestations of nonlinear optical dynamics under a single “roof.” We reviewed the theory and simulation of the byproducts accompanying optical filamentation, and showed that a unified approach is indeed possible. Employing the angularly resolved spectrum, or $K - \Omega$ spectrum, a notion that has been used to great effect in the area of nonlinear conical waves, we demonstrated that a unified approach to the byproducts accompanying optical filamentation can be achieved using the twin notions of the Effective Three-Wave-Mixing (ETWM) picture of wave-mixing in the presence of filaments, which determines the locus of phase-matched wave generation in the angularly resolved spectrum, and the first-Born approximation to determine the profile of the angularly resolved spectrum. We have shown that unlike the essentially non-perturbative core of the filament, several byproducts of filamentation can be treated as perturbative effects that have negligible feed-back effects on the filament itself. This should be of great utility for future studies of optimization of the yield of a given byproduct.

Supercontinuum generation dependence on dimensionality of the “diffraction space”

Planar glass-membrane fibers: Case of one-dimensional diffraction

Planar glass membrane fibers (PGMFs) are of current interest owing to the fact that they combine the interesting dispersive properties of fibers with diffraction in one unbound transverse dimension. We studied the supercontinuum (SC) spectra generated in PGMFs and showed that the underlying dynamics has similarities to that in bulk medium. At the

same time, the rich dispersion properties of PGMFs open up new possibilities, including SC spectral shapes that do not occur in natural bulk media. In all cases, the SC spectra in PGMFs can be interpreted in detail using the effective-three-wave-mixing model originally developed for bulk media.

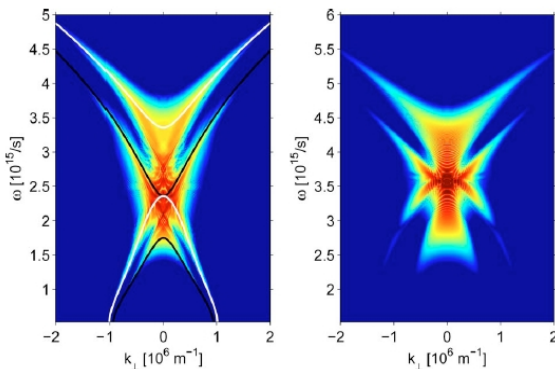


Fig. 1. (Color online) Angularly resolved (log scale) spectrum from a 600-nm-thick silica PGMF for a TE-polarized pulse of 60 fs duration and center wavelength 800 nm, resulting in an X-shaped spectrum. For comparison, the right panel shows supercontinuum generated in water ($\lambda=527$ nm, 80 fs, $4 \mu\text{J}$, 3 cm distance).

The following Figure illustrates the similarity in the shape of angularly resolved supercontinuum spectra in a bulk material (water) and in a glass-membrane which has the thickness chosen such that the TE mode propagates in a normal GVD regime. In both cases we can observe characteristic X-features well known from the bulk media. Knowing the linear chromatic properties of the medium, in this case of the planar glass membrane waveguide, one can utilize the Effective Three-Wave Mixing approach to analyze the spectrum. This provides us with the information about the parameters of the pulse splitting event which was responsible for the observed spectrum.

The next picture illustrates the similarity for the case of anomalous GVD regime. Again, the characteristic fish-like spectral form occurs in both cases as expected for the anomalous regime. The elliptic feature represents the spectrally broadened excitation wavelength which propagates in the anomalous GVD regime and therefore exhibits O-like texture, sometimes referred to as an O-wave. The angularly wide portion of the spectrum at high frequencies is a conical emission which occurs in the normal GVD range. Apart from the angular resolution made possible by the availability of diffractive dimension in the planar waveguide, these two components of the spectra, normal and anomalous are characteristic in supercontinuum generation in microstructured fibers, where the normal-GVD component is termed the dispersive wave. We can thus see that this case shares attributes of both the bulk and fiber supercontinuum dynamics.

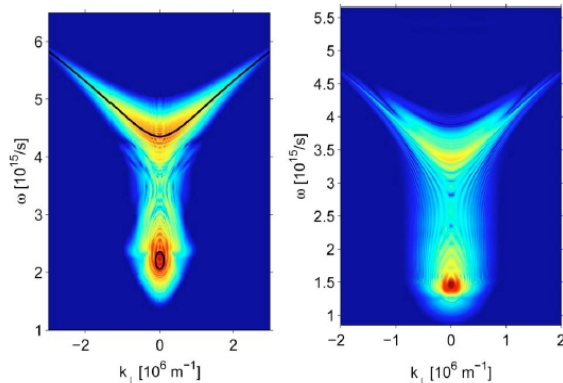
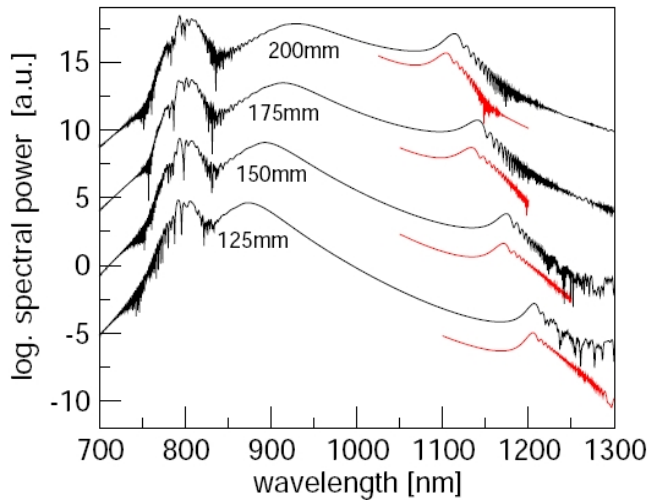


Fig. 2. (Color online) Angularly resolved spectrum generated in a 1000-nm-thick silica PGMF for a TM-polarized pulse of 30 fs duration and center wavelength 800 nm, resulting in a fishlike-shaped spectrum. For comparison, a similar spectrum generated in water ($\lambda=1300$ nm, 80 fs, $8 \mu\text{J}$, 1 cm distance) is shown in the right panel.

The important lesson learned from this study is that even “small amount of diffraction” which occurs in a single effective dimension in a planar waveguide is sufficient to make the supercontinuum generation dynamics practically equivalent to that in bulk media. Thus, while these exotic fibers can be considered an intermediate case between the bulk and “standard” microstructure fibers, from the point of view of white light generation we have shown that they should be considered much closer to the bulk.

Microstructured fibers: Case of zero-dimensional diffraction

Naturally, the previous result for planar waveguides begs the question if the theory of supercontinuum generation from bulk can be applied even to microstructured fibers with a micron-size core, i.e. to a system where diffraction does not play a role. Traditionally, the respective theories of supercontinua in fibers and in the bulk evolved without much interaction between the respective research communities. It is therefore important to explore the possibilities to draw the two closer together. With this aim, we studied the



possibility of application of the ETWM paradigm, originally developed for the bulk media, to fibers. In particular, we asked the question if the dispersive waves generated by soliton-like pulses in fibers, can be described in terms of the ETWM scattering model. We have found that this is indeed the case, and even succeeded in obtaining an analytic approximation, based on the bulk-media supercontinuum approach, which describes the dispersive wave component of fiber white light spectrum. The above picture compares the full simulation of such a spectra for increasing propagation distances in a

micron-sized core of a fiber to the analytic formula shown in red. One can see that the agreement is extremely good, which indicates that similar to bulk media, at least this portion of the white light generation can be indeed described in terms of a perturbative scattering process in which the generated light becomes completely decoupled from the high-intensity of the driving pulse-core.

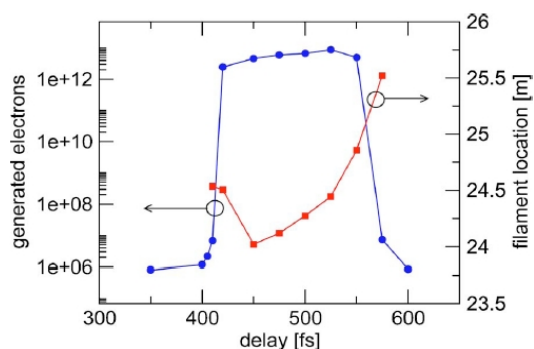
Long-distance control of femtosecond filaments.

This section briefly summarizes our results on control of various aspects of femtosecond light strings in gaseous media. For example, we show how achieving self-focusing collapse at a chosen target distance is possible through double-pulse interaction. Aspects of the linear properties of high-power beams which can be used to affect multiple filamentation regimes are also discussed.

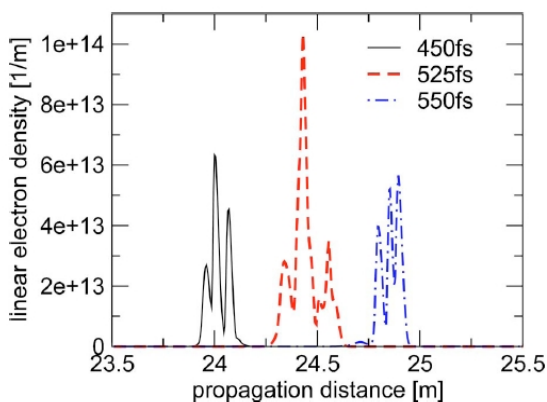
Conditional femtosecond pulse collapse for white-light and plasma delivery to a controlled distance

A great deal of effort has been going into control of filamentation and white-light generation in high-power femtosecond pulses in gases, condensed media, and fibers alike. For remote sensing applications the control of the filamentation-onset distance is of paramount importance. Based on our simulation studies, we proposed a solution based on “collision” of two, different-color pulses.

The idea is simple in principle: Suitable focusing and relative temporal delays are imposed on two sub-critical pulses with different colors, such that the group velocity dispersion causes them to “collide” in a predetermined distance. Together, pulses form a supercritical waveform which succumbs to a self-focusing collapse. As a result, high intensity and plasma are “delivered” accurately on the target.



The following Figure illustrates the on-off control of the remote filament through settings of relative pulse delay. The left hand side axis shows that free electrons are generated only for a sharply defined range of delays – this happens when both pulses “meet” and have sufficiently high intensity at the same time. The axis on the right shows the location of the created filament. The slope of the curve indicates that the precise location can be accurately controlled, and the next Figure shows that the plasma channel is well localized. Thus, one can generate plasma, right at the distant surface of a target.



In summary, we have demonstrated that spatial and temporal focusing can be effectively combined with dual-pulse excitation to achieve conditional collapse and, consequently, filament formation at a predetermined distance. The method thus allows one to control accurately if and at what distance plasma and white light are produced. These results should be useful for both remote sensing and control of filamentation and

supercontinuum generation in general.

The role of linear power partitioning in beam filamentation

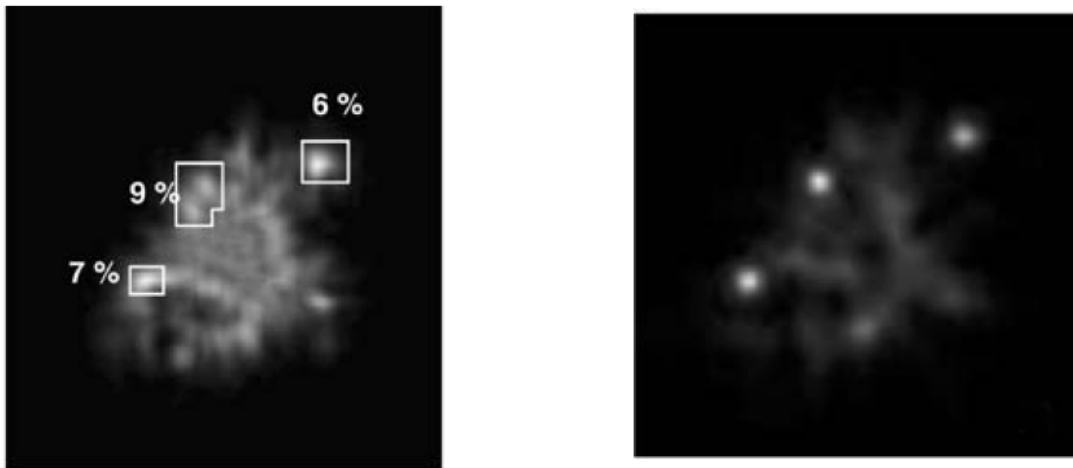
One of the outstanding questions in the field of extreme power ultrashort pulses is control of multiple filament locations. While control of a single filament is difficult already, the highly nonlinear dynamics manifest itself even more violently in wide-beam, high power situations. A lot of work in the light-string community is devoted to the problem of at least partial control.

Because it is clear that linear properties afford better opportunities to shape and design the light beams than trying to manage them in the fully developed nonlinear regime, we have posed a fundamental question, namely to what degree are the locations of multiple filaments in a high-power pulse determined by the linear “preparation” of the beam?

In our previous work published in Physical Review Letters, we introduced the idea of weak intensity background or reservoir in multi-filamentation regime and made a point that a turbulent dynamics develops in which filaments are created and decay in a chaotic, unpredictable fashion. Here we are interested if such a behavior can be beaten at least in the initial stage.

Our results, based on analysis combined with numerical investigations, indeed showed very clearly that the answer to the above question is affirmative. We have formulated the so called linear partitioning paradigm, which says that the first filament formation loci are only determined by the linear propagation properties of the initial beam. Roughly speaking, if a purely linear propagation would result in occurrence of local energy concentration in the transverse cross-section such that the power is locally super-critical, this place will give rise to “first” filament in the nonlinear regime.

Picture on the left illustrates the linear-power partitioning prediction for location of three



filaments. On the right, a fully nonlinear simulations confirm the expectation. While the fine-scale structure of the nonlinear beam is rather different from the linear one, the hot spots shape is almost completely given by the linear propagation.

We have also shown that this is true not only in the CW regime, but also for ultra-short pulses. Our results indicate that both, apertures and aberrations can be both utilized to control the placement of hot spots in high power beams.

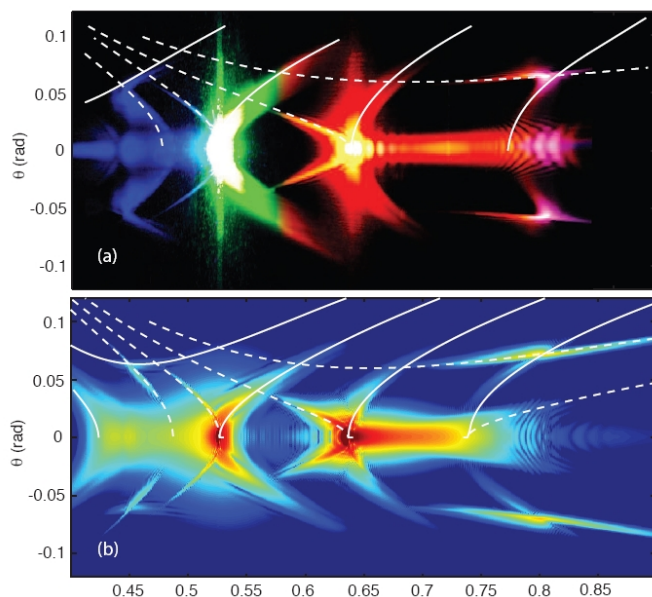
Dynamics of high-power femtosecond pulses.

This section summarizes our achievements in detailed understanding of the dynamics in high-power optical pulses that underlines white light, harmonic generation, and femtosecond filamentation. Techniques which can be applied to extract quantitative information to characterize the nonlinear processes occurring within the filament “focal volume” are studied together with ways to control spectral and temporal dynamics.

Spatio-temporal reshaping and X-Wave dynamics in optical filaments

In a joint theoretic-experimental work in collaboration with the Virtual institute of Nonlinear Optics (P. diTrapani and D. Faccio group) we investigated the dynamics of femtosecond filaments in condensed media. Water and ethanol were chosen as “model” media with the aim to “map” in detail the temporal sequence of the processes within a filament core that are responsible for phenomena such as white-light and conical emission.

We have tested the Effective Three-Wave Mixing paradigm developed previously by us, and showed that it can be applied to real-world experiments. The central working tool of this work was the angularly resolved far-field spectrum. We demonstrated that even a far-field spectrum with a complicated structure can be interpreted in detail based on ETWM. An example of such analysis is shown in the Figure. Based on the theory we developed, we can “read” the experimental angular spectrum shown in the top panel: It reflects the following sequence of events occurring within the tiny filament core. First a pump pulse undergoes self-focusing followed by temporal pulse splitting which in turn creates the X-shaped structure in the spectrum. Then, the cross-phase modulation reshapes the probe pulse tuned around the Raman resonance for the given medium. This energy is subsequently “scattered” into “conical rainbows”, the process being controlled by the



speed of temporal pulse splitting in the pump. The ETWM theory then specifies the expected location of energy concentration in the angle-frequency space, which are marked in the figure. An important result of this work is also a detailed comparison of the simulated (bottom panel) and experimental (top) far-field spectra. It is fair to say that **ours is to date the most accurate comparison in the field of filamentation in condensed media.** Clearly, the model simulated by our Unidirectional Pulse Propagation Equation solver captures spectral structures over several orders of magnitude and in an extremely wide spectral range.

Generation and control of extreme blue-shifted continuum peaks in optical Kerr media

Control of filamentation and white-light generation is crucial for further progress in extreme nonlinear optics. This motivated our work briefly described in what follows next. We demonstrated **tunable, extremely blue-shifted continuum** in ≈ 1.055 micron ultrashort laser pulse filamentation in silica. Close to threshold, the continuum appears as a single,

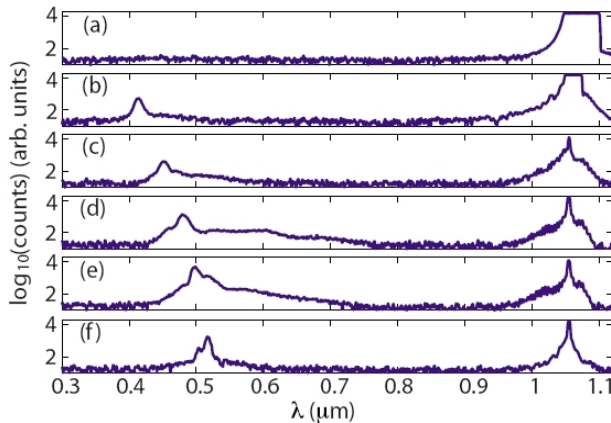


FIG. 4. (Color online) Spectra measured for different positions of the fused sample with respect to the input focusing lens. (a) 49 cm, (b) 50 cm, (c) 51 cm, (d) 52.5 cm, (e) 53 cm, and (f) 54 cm.

isolated blue peak. The spectral position of the main supercontinuum components can be tuned, and a regime with encompassing fundamental and second harmonic is possible to achieve. At higher energies, the continuum expands in bandwidth starting from the blue peak.

Consequently, we have demonstrated means to control both the location, and width of the newly generated spectral components. This is illustrated in the Figure, which shows how the central wavelength of the blue peak in the supercontinuum can be controlled via adjustment of the focal length.

We explained this spectral dynamics and tunability in terms of X-wave generation and intra-filament pulse splitting which may be controlled by modifying the input pulse focusing conditions. These insights were gained through extensive numerical simulations supported by our UPPE solver.

Our model faithfully captured the behavior of the extreme blue spectral peak. This is documented in the following Figure which shows the behavior of the extreme-blue spectral peak in the extended supercontinuum: Here we can “target” the second-harmonic spectral range by simply adjusting the beam size through the focusing lens. In this way, a very much desired supercontinuum can be created which exhibits strong components at both fundamental and second harmonic, which in turn is important for frequency combs.

Our simulations further revealed the temporal and spatial structure of the light carried by the blue peak we control.

It turns out that this part of the spectrum has properties favorable for compression, which can be used in not only new wavelength generation but also in production of ultrashort pulses. Our result thus will be of fundamental importance for optimizing energy transfer to specific wavelengths and bandwidths according to specific needs, e.g., ultrashort pulse generation, white light spectroscopy or optimized Carrier-Envelope-Offset monitoring in $f - 2f$ setups.

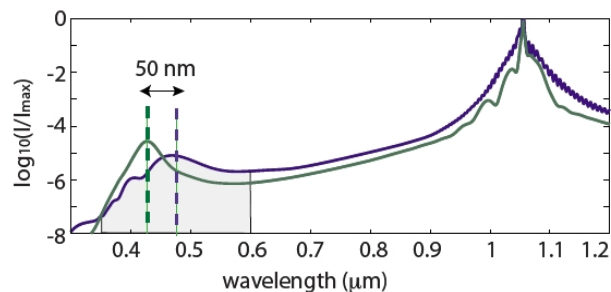
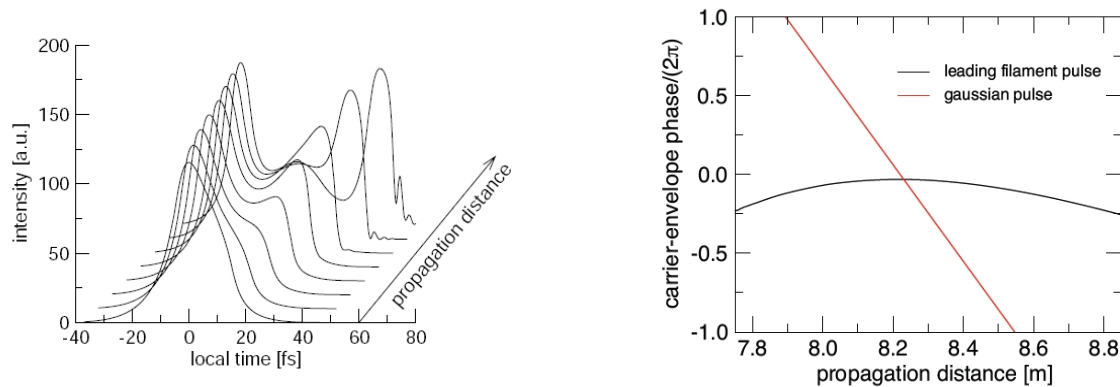


FIG. 7. (Color online) Numerically calculated on-axis spectra for two different input beam diameters: 5 mm green solid line and 3.3 mm blue dashed line. The vertical lines indicate the 50 nm wavelength shift of the blue peak.

Spontaneous emergence of pulses with constant carrier-envelope phase in femtosecond filamentation

Extending the theme of control further, we investigated if filamentation can be actually used as a tool to spontaneously create “ready-to-use” femtosecond pulses with desirable properties. This work was motivated in part by our previous publication in Physical Review Letters which identified the X-wave dynamics as the fundamental reason why filaments “hold together” and can propagate over distances longer than corresponding to their size. That work implied that if we could switch off the nonlinearity instantly, the filament would nevertheless continue to exist for a significant distance. Here we take this further, and ask if at the same time it is possible to “prepare” the resulting pulse in such a way that the carrier-envelope phase is controlled.



The picture on the left illustrates the mechanism of pulse splitting which creates two daughter pulses. The leading pulse can exhibit a nearly constant Carrier-Envelope-Phase (CEP). This is shown on the right, where we compare the CEP evolution in such a pulse to that in a Gaussian pulse. We can see that it is possible to achieve a very slowly changing CEP over a distance of several tens of centimeters. This is a very long distance, an order of magnitude better than what can be obtained from a Gaussian pulse under optimal conditions.

In summary, we have shown that pulses with constant CEP $\psi(z)$ during propagation may be created spontaneously in optical filaments. Clearly, the condition of $\psi(z)$ constant is not achievable with standard Gaussian-like pulses in dispersive media due to the necessarily different phase and group velocities. On the contrary, the X-wave nature of the filament pulses accounts for the varying group velocities that may in certain cases be equal or very close to the carrier wave phase velocity.

The conditions for the observation of constant CEP pulses have been found both in gases and highly-dispersive condensed media, thus highlighting the generality of this effect. The propagation distance over which the CEP varies by less than $\pi / 8$ is typically an order of magnitude greater than for a Gaussian pulse. In view of possible applications, it will be important to understand if it is possible to generate the constant-CEP, propagating waveforms without pedestals and satellite pulses. In particular, ways to eliminate the trailing peak and/or reduce the pulse durations should be investigated in the future.

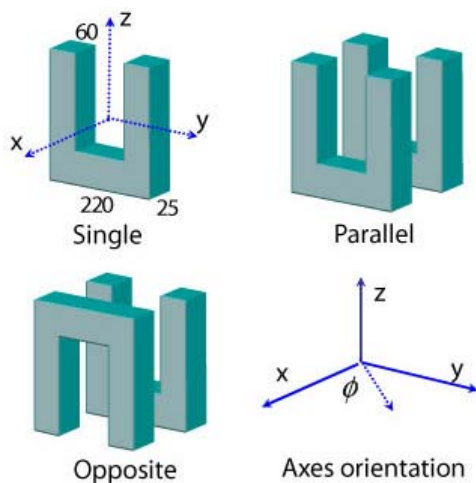
The role of magnetic dipole moments in Metamaterials

Metallic split ring resonators (SRR) arrays are a popular building block for metamaterials and have attracted intensive attention in the last decade. Such arrays are sometimes referred to as magnetic metamaterials due to the role played by magnetic dipoles in their optical response. However, due to the difficulty in experimentally measuring nanoscale magnetic dipoles the role of magnetic dipoles is unclear or even over emphasized in the literature. The aim research carried out under Grant/Contract Number: FA9550-07-1-0010 was to clarify the role of magnetic dipoles by numerically computing their magnitude and examining their relative contributions to the scattering cross section.

Using custom finite-difference time-domain (FDTD) code and a new near-to-far-field transformation algorithm developed at the ACMS we numerically computed electric and magnetic dipole moments of various SSR configurations and performed a quantitative analysis of their relative contributions to the scattering cross section. We also studied the role of magnetic dipoles and higher order multipoles in second harmonic generation.

Numerical modeling

Experimentally single- and multi- layered metallic single-slit SRR membranes have been fabricated and their optical responses are usually studied by measuring their transmission spectra at normal incidence. A magnetic dipole moment perpendicular to the membrane, arising from a current circulating inside the SRR, is frequently mentioned as having a role in the observed transmission spectrum and in the coupling between adjacent SRRs. However direct experimental measurement of magnetic dipoles in these nanoscale structures is difficult. Furthermore, rarely mentioned is the contribution from a magnetic dipole parallel to the incident magnetic field arising from the strongly localized conduction electrons near the metallic surfaces.



To numerically investigate the effects of magnetic dipoles and to we developed a new near-to-far-field transformation algorithm for FDTD based directly on the polarization current of the metallic scatterer that eliminates the numerical errors due to spatial offset of the E and H fields. To study second-harmonic radiation from individual SRRs, as schematically shown in the Figure, we developed a new *classical* electrodynamic theory to study the optical nonlinearities of metallic nanoparticles. Our three dimensional finite-difference time-domain approach, even without an accurate treatment of the surface electrons, qualitatively captures the dominant physical mechanisms of second-harmonic generations from metallic nanoparticles.

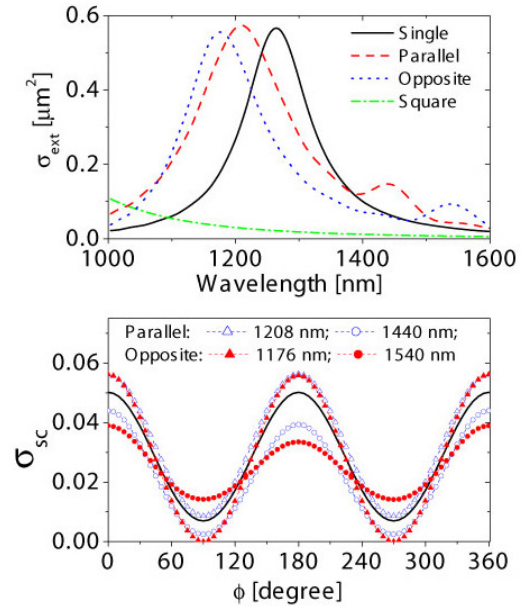
Through detailed experiment-theory comparisons, we validate this classical theory as well as the associated numerical algorithm. It was demonstrated that our theory not only provides qualitative agreement with experiments but it also reproduces the overall strength of the experimentally observed second-harmonic signals.

A practical outcome from our numerical simulations is a proposed experimental

configuration by which the strength of magnetic dipoles can be determined experimentally by measuring the scattering cross section along particular directions. The Figure shows the computed absolute extinction cross section σ_{ext} and differential scattering cross section σ_{sc} of split-ring resonator configurations considered in the study as a function of the azimuthal angle ϕ .

We also show that in certain configurations the magnetic dipole parallel to the membrane plays a significant role. For isolated pairs of coupled SRRs high-order multipoles contribute considerably to the scattering cross section and we numerically verify that the magnetic dipole-dipole interaction must be considered to interpret the coupling strength between coupled SRRs.

We also note that the electric dipole-dipole interaction dominates the coupling between adjacent SRRs, and that the magnetic dipole-dipole interaction is responsible for an increased resonance separation in the anti-symmetric (opposite) configuration shown in the figure.



PUBLICATIONS: 2006

Y. Xie, A. R. Zakharian, J. V. Moloney, and M. Mansuripur, "Transmission of light through periodic arrays of sub-wavelength slits in metallic hosts", *Optics Express*, **14**, 6400, 2006.

A. R. Zakharian, P. Polynkin, M. Mansuripur, and J. V. Moloney, "Single-beam trapping of microbeads in polarized light: Numerical simulations," *Opt. Express*, **14**, 3660, 2006.

M. Kolesik, E.M. Wright, A. Becker and J.V. Moloney, "Simulation of third-harmonic and supercontinuum generation for femtosecond pulses in air", *Applied Physics B*, **85**, 531, 2006.

A.R. Zakharian, M. Brio, C. Dineen, and J.V. Moloney, "Stability of 2D FDTD Algorithms with Local Mesh Refinement for Maxwell's Equations", *Communications in Mathematical Sciences*, **4**, 345, 2006.

A.R. Zakharian, M. Brio, C. Dineen and J.V. Moloney, "Second-Order Accurate FDTD Space and Time Grid Refinement Method in Three Space Dimensions", *IEEE Photonics Technology Letters*, **18**, 1237, 2006.

M. Kolesik, E.M. Wright, A. Becker and J.V. Moloney, "Simulation of third-harmonic and supercontinuum generation for femtosecond pulses in air", *Applied Physics B*, **85**, 531, 2006.

PUBLICATIONS: 2007

Armis R. Zakharian, Jerome V. Moloney, and Masud Mansuripur, "Surface Plasmon Polaritons on Metallic Surfaces", *IEEE Transactions on Magnetics*, **43**, 845, 2007.

M. Kolesik, D. Roskey, and J.V. Moloney, "Conditional femtosecond pulse collapse for white-light and plasma delivery to a controlled distance", *Optics Letters*, **32**, 2753, 2007.

M. Kolesik, E.M. Wright, and J.V. Moloney, "Supercontinuum and Third-Harmonic Generation accompanying Optical Filamentation" as First-Order Scattering Processes *Optics Letters*, **32**, 2816, 2007.

D. Faccio, A. Averchi, A. Couairon, M. Kolesik, J.V. Moloney, A. Dubietis, G. Tamosauskas, P. Polesana, A. Piskarskas, P. Di Trapani, "X wave generation by Cross-Phase-Modulation induced spatio-temporal reshaping and amplification within optical filaments", *Optics Express*, **15**, 13077, 2007.

D. Roskey, M. Kolesik, J.V. Moloney, and E.M. Wright, "Self-action and regularized self-guiding of pulsed Bessel-like beams in air", *Optics Express*, **15**, 9893, 2007.

D. E Roskey, M. Kolesik, J. V Moloney and E. M Wright, "The role of linear power partitioning in beam filamentation" *Applied Physics B*, **86**, 249, 2007.

D. Faccio, A. Averchi, A. Couairon, M. Kolesik, J.V. Moloney, A. Dubietis, G. Tamosauskas, P. Polesana, A. Piskarskas, P. De Trapani, "Spatio-temporal reshaping and X Wave dynamics in optical filaments", *Optics Express Vol. 15*, No. 20, 13077, October 2007.

PUBLICATIONS: 2008

Reichelt, M.; Dineen, C.; Koch, S.W.; Moloney, J.V, "Optical Forces on a Quantum Dot in Metallic Bowtie Structures", *Photonics Technology Letters, IEEE*, Volume **20**, Issue 6, March 15 Page(s):431 – 433, 2008.

M. Kolesik, J. V. Moloney, "Perturbative and non-perturbative aspects of optical filamentation in bulk dielectric media", *Optics Express, Focus Issue: Frontiers of Nonlinear Optics*, **16**, 2971, March 2008.

D. Faccio, A. Lotti, M. Kolesik, J.V. Moloney, S. Tzortzakis, A. Couairon, P. Di Trapani, "Spontaneous emergence of pulses with constant carrier-envelope phase in femtosecond filamentation", *Optics Express*, Vol. **16**, No. 15, 11103, July 2008.

Shuqi Chen, Lin Han, Axel Schülzgen, Hongbo Li, Li Li, Jerome V. Moloney, and N. Peyghambarian "Local electric field enhancement and polarization effects in a surface-enhanced Raman scattering fiber sensor with chessboard nanostructure", *Optics Express* Vol. **16**, No. 17, 13019, August 2008.

N. Feth, S. Linden, M. W. Klein, M. Decker, F. B. P. Niesler, Y. Zeng, W. Hoyer, J. Liu, S. W. Koch, J. V. Moloney, and M. Wegener, "Second-harmonic generation from complementary splitting resonators", *Optics Letters*, Vol. **33**, No. 17, September, 2008

P. Polynkin, M. Kolesik, A. Roberts, D. Faccio, P. Di Trapani, J.V.Moloney, "Generation of extended plasma channels in air using femtosecond Bessel Beams", *Optics Express*, Vol. **16**, No. 20, 15733, September 2008.

Averchi, D. Faccio, R. Berlasso, M. Kolesik, J.V. Moloney, A. Couairon, and P. Di Trapani, "Phase matching with Pulsed Bessel Beams for High-order Harmonic Generation", *Phys. Rev. A*, **77**, 021802, February 2008.

D. Faccio, A. Averchi, A. Lotti, M. Kolesik, J. V. Moloney, A. Couairon, and P. Di, "Generation and control of extreme blueshifted continuum peaks in optical Kerr media", *Physical Review A* **78**, 033825, September 2008.

Shuqi Chen, Weiping Zang, Axel Schulzgen, Jinjie Liu, Lin Han, Yong Zeng, Jianguo Tian, Feng Song, Jerome V. Moloney, and Nasser Peyghambarian, "An implicit high-order unconditionally stable complex envelope algorithm for solving the time-dependent Maxwell's equations", *Optics Letters*, Vol. **33**, Issue 23, pp. 2755-2757 (2008).

PUBLICATIONS: 2009

Liu, J., Brio, M., and Moloney, J. V. 2009. "Overlapping Yee FDTD Method on Nonorthogonal Grids". *J. Sci. Comput.* **39**, 1, pp129-143, Apr. 2009.

M. Kolesik, D. Faccio, E.M. Wright, P. Di Trapani, J.V. Moloney, "Supercontinuum generation in planar glass membrane fibers: Comparison with bulk media", *Optics Letters*, Vol. **34** Issue 3, pp.286-288 (2009).

Yong Zeng and Jerome V. Moloney, "Polarization-current based, finite-difference time-domain, near-to-far-field transformation", *Optics Letters*, Vol. **34**, p 1600-1602, 2009.

Y. Zeng, W. Hoyer, J. Liu, S. W. Koch, and J. V. Moloney, "A classical theory for second-harmonic generation from metallic nanoparticles", *Physical Review B*, Vol. **79**, 2009.

Jinjie Liu, Moysey Brio, Jerome V. Moloney, "A diagonal split-cell model for the overlapping Yee FDTD method", *Acta Mathematica Scientia*, Volume **29**, Issue 6, Pages 1670-1676, ISSN 0252-9602, 2009

Jakobsen, Per, "Calculating optical forces using the boundary integral method", *Physica Scripta*, Volume **80**, Issue 3, pp. 035401 (2009).

PUBLICATIONS: 2010

Y. Zeng, C. Dineen, and JV Moloney, "Magnetic dipole moments in single and coupled split-ring resonators," *Phys. Rev. B* **81**, 075116 (2010)

D. Faccio, S. Cacciatori, V. Gorini, V. G. Sala, A. Averchi, A. Lotti, M. Kolesik, J. V. Moloney, "Analogue gravity and ultrashort laser pulse filamentation", *Europhysics Letters* **89**, 34004 (2010)

Jinjie Liu, Moysey Brio, Yong Zeng, Armis R. Zakharian, Walter Hoyer, Stephan W. Koch, Jerome V. Moloney, "Generalization of the FDTD algorithm for simulations of hydrodynamic nonlinear Drude model", *Journal of Computational Physics*, Volume **229**, Issue 17, 20, Pages 5921-5932, August 2010

Conference Proceedings:

P. Polynkin, M. Kolesik, J. Moloney, G. Siviloglou, D. Christodoulides, "Filamentation of femtosecond self-bending Airy beams", Conference on Lasers and Electro-Optics/International Quantum Electronics Conference, Ultrafast Lasers, Precision Optical Metrology, Fibers and Guided Waves, CPDB, CPDB11, Baltimore, Maryland, 2009.

Talks (invited and contributed):

Invited talk J.V. Moloney, at SIAM , Rome, Italy "Perturbative and Nonperturbative Aspects of Ultra-short Pulse Filamentation", July 2008

Jinjie Liu, "Nonorthogonal overlapping Yee FDTD method with application to optical force computation", Modeling and Computation Seminar, Department of Mathematics, The University of Arizona, Tucson, AZ, September 18, 2008.

Yong Zeng, "A classical model of second-harmonic generation from metal-based metamaterials", Modeling & Computation Seminar, Department of Mathematics, University of Arizona, October 2, 2008.

Miroslav Kolesik, "Extreme nonlinear optics: from models and simulations to understanding physics", California State University Long Beach, Physics and Astronomy Department, January 25, 2009.

Jinjie Liu, "Nonorthogonal Overlapping Yee FDTD Method and Applications", Department of Mathematics, City University of Hong Kong, Hong Kong, February 17, 2009.

J.V. Moloney, Ultrafast Nonlinear Optics: Manipulating plasma channels using Bessel and Airy beams" colloquium talk at San Francisco State University, March 9, 2009.

Jinjie Liu, "Nonorthogonal Overlapping Yee FDTD Method and Applications", Department of Applied Mathematics and Theoretical Physics, Delaware State University, Dover, Delaware, April 20, 2009.

Miroslav Kolesik, STELLA 2009 Summer School, Simulational nonlinear optics, Casteldefels (Barcelona), Spain, April 20 - 30, 2009.

J.V. Moloney, "Ultrafast nonlinear optics: Manipulating plasma channels using Bessel and Airy beams", invited seminar at the Tyndall national Institute, Cork, Ireland, May 25, 2009.

J.V. Moloney, "Computational Nanophotonics/Plasmonics and Metamaterials", invited seminar at the Tyndall National Institute Cork, Ireland, June 4, 2009.

Jinjie Liu, Moysey Brio, and Jerome V. Moloney, "Overlapping Yee FDTD Method on Nonorthogonal Grids", 2009 SIAM Annual Meeting, Denver, Colorado, July 6-10, 2009.

Yong Zeng, "A Classical Study of Second-Harmonic Generation from Metallic Nanoparticles", Nonlinear Optics Topical Meeting, Honolulu, Hawaii, July 15, 2009.

Jinjie Liu, Moysey Brio, and Jerome V. Moloney, "Overlapping Yee FDTD Method on Nonorthogonal Grids", National Congress on Computational Mechanics, Columbus, Ohio, July 16-19, 2009.

J.V. Moloney, Invited talk at NLO contractor's meeting, "Fundamental Modeling and Design Strategies in Computational Photonics: Applications to Lasercom through clouds and Electro-optical/ Nanophotonics", Dayton, Ohio, September 9, 2009.

J.V. Moloney, "Ultrashort Intense Pulse Propagator: Light Strings, Higher Harmonic Generation and Extreme NLO", invited talk at NLO contractor's meeting, Dayton, Ohio, September 9, 2009.

P. Polynkin, "Experiments on Filamentation of Beam-Shaped Femtosecond Laser Pulses in Gases and Liquids", invited talk at NLO contractor's meeting, Dayton, Ohio, September 9, 2009.

Interactions/Transitions:

Our key results were presented at a recent contractor's review meeting at AFRL Wright-Patterson, Dayton by the Principal Investigator.

We are teaming up with Dr. William P. Roach and Richard Albanese at Brooks AFB who have internal funding to study the feasibility of coupling of RF and HPM energies to femtosecond pulse generated plasma channels.